Geomechanics and Engineering, *Vol. 21, No. 2 (2020) 153-164*
DOI: https://doi.org/10.12989/gae.2020.21.2.153

Determination of effective parameters on surface settlement during shield TBM

Dongku Kim[1b], Khanh Pham[1a], Sangyeong Park[1b], Ju-Young Oh[2a] and Hangseok Choi*[1]

[1]*School of Civil, Environmental and Architectural Engineering, Korea University, 145 Anam-ro, Seongbuk-gu, Seoul, Republic of Korea*
[2]*Infrastructure ENG Team, Infra Construction ENG Group, Samsung C&T, 500 Sangil-ro, Gangdong-gu, Seoul, Republic of Korea*

(Received December 11, 2019, Revised March 1, 2020, Accepted March 2, 2020)

Abstract. Tunnel excavation in shallow soft ground conditions of urban areas experiences inevitable surface settlements that threaten the stability of nearby infrastructures. Surface settlements during shield TBM tunneling are related to a number of factors including geotechnical conditions, tunnel geometry and excavation methods. In this paper, a database collected from a construction section of Hong Kong subway was used to analyze the correlation of settlement-inducing factors and surface settlements monitored at different locations of a transverse trough. The Pearson correlation analysis result revealed a correlation between the factors in consideration. Factors such as the face pressure, advance speed, thrust force, cutter torque, twin tunnel distance and ground water level presented a modest correlation with the surface settlement, while no significant trends between the other factors and the surface settlements were observed. It can be concluded that an integrated effect of the settlement-inducing factors should be related to the magnitude of surface settlements.

Keywords: shield TBM tunneling; surface settlement; effective parameter; Pearson correlation; twin tunnel

1. Introduction

Growing demand for underground transportation in urban areas has increased excavation of subway tunnels in shallow ground conditions. Many of these tunnels are constructed in a complex underground condition where tunneling-induced ground movement has a high probability of causing serious damage to existing structures. To prevent such risk, a reliable estimation of the magnitude of surface settlement should be made, at the design stage using appropriate methods.

Numerous researchers have attempted to predict the surface settlement in various approaches. Analytical solutions have limitations in predicting settlements of actual construction site due to the complex and nonlinear relationships, and interactions between effective parameters on surface settlement (Loganathan and Poulos 2002, Park 2005, Sagaseta 1987, Verruijt and Booker 1998). Some of the limitations result from oversimplifications such as the plain strain, elastic behavior and isotropy condition. Empirical solutions have been generally adopted based on the data obtained from field observation by monitoring actual tunnel projects (Atkinson and Potts 1977, Attewell *et al.* 1986, Ding and Wei 2017, Mair 1983, O'Reilly and New 1982, Peck 1969). Relatively accurate estimations of surface settlement can be acquired from extensively detailed numerical models (Ding *et al.* 2004, Eskandari *et al.* 2018, Kasper and Meschke 2004, Kim *et al.* 2018, Melis *et al.* 2002, Razaei *et al.* 2019). However, numerical modeling processes are time-consuming and challenged to handle assumptions induced by a lack of ground information.

Artificial intelligence methods have been introduced to address the relationship between the magnitude of surface settlements and the effective parameters on surface settlements. In the early research stages, Artificial Neural Networks (ANNs) have been employed, showing the applicability of artificial intelligence methods (Kim *et al.* 2001, Neaupane and Adhikari 2006, Santos and Celestino 2008, Suwansawat and Einstein 2006, Yagiz *et al.* 2009). As shown in Table 1, the effective parameters adopted in these studies are diverse, primarily because of distinct tunnel construction conditions. Although multiple researches suggested settlement-inducing parameters to be categorized into three groups, i.e., geometric conditions, geological conditions and excavation conditions, different numbers and kinds of settlement-inducing parameters are being adapted in the previous studies.

In recent studies, various types of ANNs and other machine learning algorithms have been employed to enhance the settlement prediction accuracy. The algorithms derived from ANN, i.e., Adaptive Neuro-Fuzzy Inference System (ANFIS), Particle Swarm Optimization (PSO)-ANN and General Regression Neural Network (GRNN) are employed to estimate settlements (Ahangari *et al.* 2015, Bouayad and Emeriault 2017, Hasanipanah *et al.* 2016, Chen *et al.* 2019). A hybrid algorithm, which integrates Support Vector Machine (SVM) and an optimization algorithm, accurately predicts the surface settlement evolution (Zhang *et al.* 2017). Application of an ensemble learning algorithm presented that Random Forest (RF) is

*Corresponding author, Professor
E-mail: hchoi2@korea.ac.kr
[a]Ph.D.
[b]Ph.D. Student

http://www.techno-press.org/?journal=gae&subpage=7
ISSN: 2005-307X (Print), 2092-6219 (Online)

Table 1 List of effective parameters in literatures

Researcher	Category	Parameters	Researcher	Category	Parameters
Kim *et al.* (2002)	Tunnel geometries	Tunnel depth Excavation width Excavation height Tunnel shape Tunnel type Pillar width	Neaupane and Adhikari (2006)	-	Depth to axis Excavated diameter Volume loss Ground water level Shear strength Construction method
	Ground conditions	Host rock mass Rock mass type and overburden Soil layer type and overburden Ground water level Ground water inflow rate	Santos and Celestino (2008)	Geometrical	Overburden Cross-section area Shotcrete thickness Chainage
				Geotechnical	Clay percentage Sand percentage Tunnel depth below the water table Average SPT in excavation
	Excavation and support conditions	Support methods Excavation methods Excavation type Auxiliary technique Supporting time Velocity of excavation Excavation length Drainage system		Excavation	Advance rate – before (10m) Advance rate – before (5m) Advance rate under section Advance rate after (5m) Advance rate after (10m) Face to invert distance
Suwansawat and Einstein (2006)	Tunnel geometry	Tunnel depth Distance from launching station	Ahangari *et al.* (2015)	-	Elasticity modulus Cohesion Angle of internal friction Tunnel diameter Tunnel depth Settlement
	Geological conditions	Geology at tunnel crown Geology at tunnel invert Ground water level from tunnel invert			
	Shield operation factors	Face pressure Penetration rate Pitching angle Tail void grouting pressure Percent tail void grout filling			

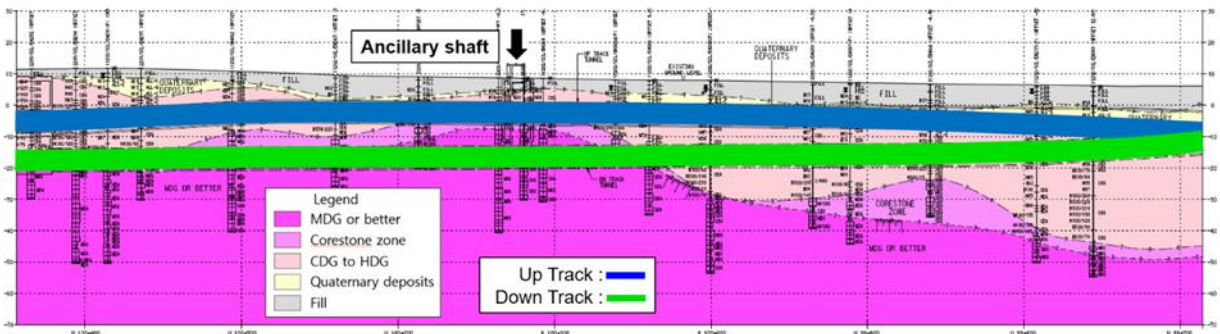

Fig. 1 Longitudinal geological profile

applicable for the prediction of surface settlements (Kohestani *et al.* 2017). Despite such prediction performances, the diversity of effective parameters utilized in each research limits the artificial intelligence methods to be put into a practical use.

The interaction of settlement-inducing parameters is neither simple nor linear. The relationship between the settlement-inducing parameters and settlement measurements recorded at the tunneling site in Hong Kong has been reviewed and analyzed. The extensive data collected from the Hong Kong tunneling site were categorized according to the recommendation of Leca and New (2007). The distribution of data, Pearson correlation coefficients and distribution of parameters were analyzed to identify the effective parameters on the surface settlement at the site in consideration.

2. Site conditions

This study examined the stacked twin subway tunnel excavated with slurry shield TBMs at Hong Kong. Two slurry shield TBMs were operated from the launching station, i.e., the up- and down-track tunnel. The down track tunnel was launched five months prior to the up-track tunnel to minimize ground disturbance. For both the up- and down-track tunnel, the outer diameter is 7.1 m, with concrete segments of 30 cm thickness and 1.5 m or 1.2 m width in the 6+1 segment configuration. The up-track tunnel was constructed in a shallow ground condition, in which the distance between the ground surface and the tunnel crown ranged from 6.74 m to 12.86 m as shown in Fig. 1. The ground water level located between 3.01 and 7.23 mPD below the ground level. The symbol of ‘mPD’

Table 2 Geotechnical conditions of the tunneling site

Ground type	Unit weight (kN/m^3)	N_{SPT}	Young's modulus (MPa)	Cohesion intercept (kPa)	Friction angle (°)	K_0	Permeability (m/sec)
Fill	19	<10	1.5 x N_{SPT}	1	35	0.4	1.45 x 10^{-5}
Alluvium	19	24~30	1.5 x N_{SPT}	1	35	0.4	5.54 x 10^{-6}
CDG	19	35~46	1.5 x N_{SPT}	8	38	0.4	3.22 x 10^{-6}
HDG	19	200	300	12	40	0.4	3.90 x 10^{-6}

Table 3 Specification of operated TBM

Description	Specification
Manufacturer	Herrenknecht
Cutting diameter	7.4 m (Segment OD 7.1 m / ID 6.5 m)
Cutter head type	Mixed ground (rock / soft ground)
Maximum thrust	47,897 kN
Maximum torque	5 MN·m
Operating slurry pressure	4.0 Bar
Backfill grout	2 part injection system

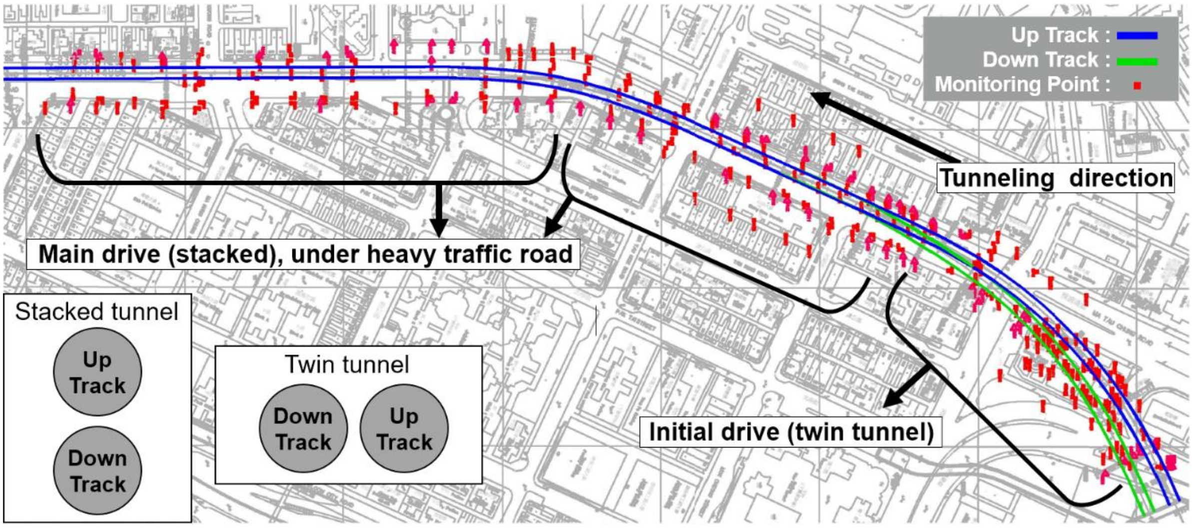

Fig. 2 Distribution of surface settlement monitoring points along tunnel alignment

means a unit of depth applied in Hong Kong, which refers to the principal datum, 1.23 m below 19-year observations of tide levels in North Point, Victoria Harbour. The tunnel, with an 850-m-driven length, was constructed under the heavy traffic road, through dense residential and commercial areas. The initial drive includes a launching process, which the TBM excavated through a 7-m-long seal-ring at the launching station. During the initial drive, the TBM drove under a park area in the twin tunnel mode with 300 m radius curves, as shown in Fig. 2. For the main drive, the tunnels were stacked each other with the up-track tunnel being located on top of the down-track tunnel. This paper analyzes the data collected from the excavation of the up-track tunnel, and the settlements monitored two months after the construction to consider the secondary settlement effect.

Geological conditions of the tunnel passage can be categorized into three layers, i.e., the fill layer, alluvial layer and decomposed granite rock layer. The fill layer is composed of loose silt and sand, and the alluvium layer is composed of alluvial clays, silts, sands and occasional gravels. According to the degree of weathering, the decomposed granite rock layer is classified as the completely decomposed granite (CDG), highly decomposed granite (HDG), moderately decomposed granite (MDG) and corestone zone. Detailed geotechnical parameters of the ground condition along the tunnel track are summarized in Table 2.

With consideration of the site condition, slurry shield TBMs, which are compatible with both rock and soft ground conditions, were employed. Bentonite slurry was applied for face supporting and carrying excavated materials, while compressed air bubbles were used to control face pressure. The cutting diameter of 7.4 m created

Table 4 Range of surface settlement-inducing parameters

Type	Description	Range				Unit
		Min	Max	Mean	Std	
Tunnel geometrical condition	Chainage	0	792	317.57	226.71	m
	Horizontal distance of settlement	-32.93	46.02	4.19	14.74	m
	Soil cover above tunnel	6.74	12.86	7.99	1.33	m
	Twin tunnel distance	0	16.77	4.81	6.08	m
Geological, geotechnical condition	Soil type of tunnel path	1	3	2.17	0.63	-
	Soil thickness of fill	1.9	7.2	5.37	1.37	m
	Soil thickness of alluvium	0	5.3	1.74	1.4	m
	Soil thickness of CDG	0	6.4	0.87	1.61	m
	Standard penetration test N-value	10	36	18.3	6.28	-
	Ground water level	3.01	7.23	4.72	1.08	mPD
	Building surcharge	0	9	0.65	1.9	kN/m^2
TBM operating condition	Face pressure	1.2	2.35	1.72	0.3	bar
	Advance speed	11	47	31.28	10.27	mm/min
	Back grout injection volume	5.8	7.4	6.51	0.31	m^3
	Thrust force	9700	27000	15595.27	3639.43	kN
	Cutter torque	0.25	1.5	0.8	0.34	MN·m
	Pitching	-31	35	4.69	25.7	mm
	Rolling	-12	8	-0.62	5.34	mm

0.3 m gaps from the outer diameter of the segment, which were filled by a bi-component injection backfill grout system. The detailed specification of the TBM is summarized in Table 3.

Surface settlements were monitored at 248 points along the up-track tunnel, at the chainage between 99+584.69 m and 100+376.69 m, a total length of 792 m. The location of settlement monitoring sensors was determined with consideration of heavy traffic of the main road, dense residential area and free-field ground conditions at the park area. For this reason, the number of settlement monitoring points in each transversal settlement array varied. The furthest settlement monitoring point was located at 46.02 m apart from the centerline of the tunnel, where careful monitoring of surface movements was required because of the old buildings in this area. Fig. 2 shows the distribution of surface settlement monitoring points along the tunnel alignment.

3. Surface settlement inducing parameters

According to the recommendation of Leca and New (2007), settlement-inducing factors for shield TBMs can be categorized as follows:

(1) Geological, hydro-geological and geotechnical conditions
(2) Tunnel geometry and depth
(3) Excavation methods
(4) Quality of workmanship and management

In this paper, the settlement-inducing parameters are categorized in accordance with the above recommendation, except for the last category because of the difficulty of evaluating the quality of workmanship and management. The geological and geometrical parameters are obtained from both laboratory and in situ tests. The TBM operation parameters were collected from the shield TBM operation reports. The database of several representative parameters was selected for analysis with consideration of earlier researches as shown in Table 4 (Ahangari *et al.* 2015, Kim *et al.* 2001, Neaupane and Adhikari 2006, Santos and Celestino 2008, Suwansawat and Einstein 2006).

For the geometrical condition of tunnels, four geometry factors were considered: chainage, horizontal distance of settlement, soil cover above the tunnel and twin tunnel distance. The Hong Kong subway tunnel shows a few distinctive zones along the tunnel passage and is represented with the chainage-length parameter, which is the longitudinal distance from the launching station. The horizontal distance of the settlement monitoring point was taken into account to consider the irregular measurement arrays. The twin tunnel distance or horizontal distance between the centerlines of each tunnel during the initial drive (i.e., twin tunnel section) was considered to represent the different characteristic of settlements from the main drive (i.e., stacked-tunnel section).

Soil types along the Hong Kong subway tunnel are divided into three categories: 1) Fill, 2) Alluvium and 3) CDG (completely decomposed granite). The layer thickness of each soil type was examined to demonstrate the effect of geological properties of each soil type. The N-value from the standard penetration test was also considered to specify the soil strength property. The ground water level was represented in mPD, the depth from the principal datum practiced in Hong Kong. The building surcharge, as a

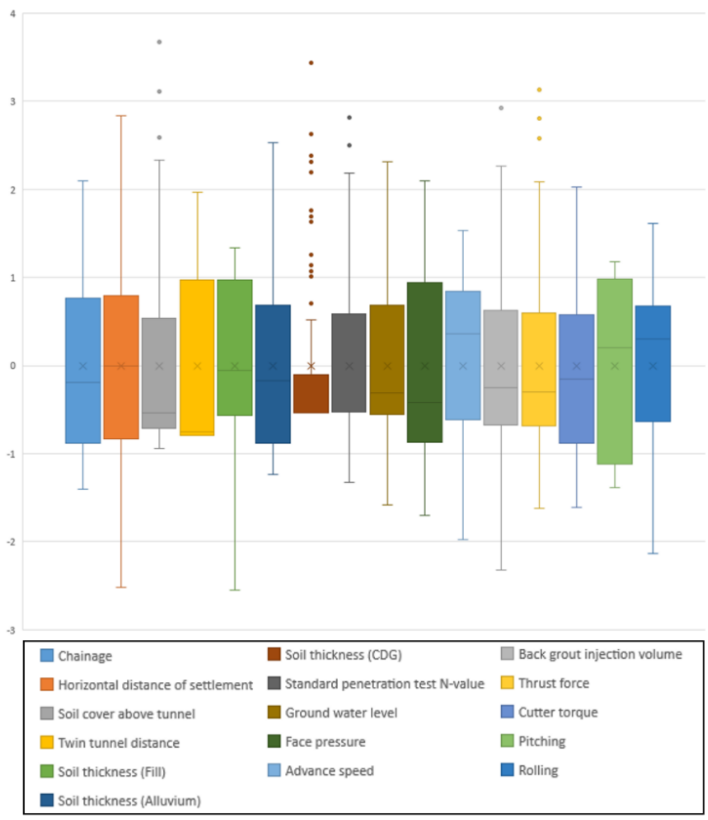

Fig. 3 Box and whisker graph of settlement-inducing parameters after standardization

unique feature of urban tunneling, was considered along with the critical vertical building surcharge in terms of K_0 value and surcharge area.

Primary control parameters relevant to slurry shield TBMs are face pressure, advance speed, back grout injection volume, thrust force, cutter torque, pitching and rolling. The face pressure is directly related with the settlements both ahead of the tunnel face and after excavation. The advance speed of a slurry shield is measured along with the net stroke distance and net excavation time for each ring. Backfill grouting pressure was not considered in this study because the backfill grouting pressure at the current site was maintained at 4 bar consistently to minimize surface settlements. Instead, the injection volume of backfill grouting was analyzed to scrutinize the relationship with the settlements induced at the tail of the TBM shield. The TBM load factors, i.e., the thrust and cutter torque, were also monitored to determine their relationship with surface settlements. The position of shield TBM, represented by pitching and rolling, indicates the annual gap at the tail of shield due to the tunnel alignment. The allowable tolerance for alignment management was set to be ±75 mm.

To show the distribution of entire database, the settlement-inducing parameters are standardized according to Eq. (1). Fig. 3 shows a box and whisker plot, representing the maximum, minimum, interquartile range, average and outliers. Parameters with discrete values such as the soil type of tunnel path and building surcharge are removed from the plot. The standardization process provides the average value of all parameters to be aligned at zero. It can be seen that the dataset is quite widely distributed and the distribution of most parameters is not symmetric. The parameter with the widest range is the horizontal distance, which also shows high normality, indicating the well-balanced surface settlement monitoring points at both sides of the tunnel centerline. The narrowest data distribution was observed in the soil thickness of CDG, which is highly skewed towards the lower value. This represents the scarcity of CDG layers along the tunnel alignment. Outlier values were detected in the five parameters according to the Tukey's rule: soil cover above tunnel, soil thickness (CDG), N-value, back grout injection volume and thrust force.

$$z = \frac{x_i - \mu}{\sigma} \tag{1}$$

where μ is the average, σ is the standard deviation.

In addition, the Pearson correlation coefficient analysis was employed to define a relationship between the settlement inducing parameters and surface settlements. The Pearson correlation measures a linear correlation relationship between two variables, where 1 indicates the total positive linear correlation and -1 indicates the total negative linear correlation. The value of zero indicates that there is no linear correlation. The Pearson correlation (r_{xy}) is calculated by the covariance of two variables divided by the product of their standard deviation as shown in Eq. (2).

$$r_{xy} = \frac{\sum_{i=1}^{n}(x_i - \bar{x})(y_i - \bar{y})}{\sqrt{\sum_{i=1}^{n}(x_i - \bar{x})^2}\sqrt{\sum_{i=1}^{n}(y_i - \bar{y})^2}} \tag{2}$$

	Chainge	Hori	Above	Twin	Type	Fill	Alluvium	CDG	N	GWL	Surcharge	FaceP	Advance	GroutV	Thrust	Torque	Pitching	Rolling	Settle
Settle	0.54	-0.08	-0.07	-0.44	0.19	-0.04	-0.16	0.12	0.08	0.58	0.18	0.49	-0.40	-0.08	0.52	0.56	-0.01	0.16	1.00
Rolling	0.51	-0.19	-0.17	-0.72	-0.11	0.21	-0.47	0.10	-0.10	0.39	0.21	0.25	-0.41	-0.56	0.09	0.13	-0.59	1.00	
Pitching	-0.10	0.17	0.64	0.63	0.54	-0.52	0.64	0.41	0.63	0.05	0.10	-0.04	0.16	0.22	0.17	0.14	1.00		
Torque	0.52	-0.06	-0.11	-0.37	0.16	0.05	-0.14	0.00	0.04	0.60	0.25	0.45	-0.38	-0.15	0.61	1.00			
Thrust	0.76	-0.06	0.22	-0.48	0.36	-0.35	0.25	0.26	0.31	0.79	0.27	0.74	-0.58	-0.10	1.00				
GroutV	-0.27	0.11	-0.03	0.32	-0.07	-0.06	0.20	-0.16	-0.08	-0.21	-0.24	-0.18	0.31	1.00					
Advance	-0.68	0.16	-0.04	0.56	-0.30	0.05	0.05	-0.12	-0.19	-0.58	-0.38	-0.74	1.00						
FaceP	0.78	-0.10	0.13	-0.54	0.45	-0.36	0.17	0.27	0.30	0.75	0.27	1.00							
Surcharge	0.36	0.00	0.01	-0.26	-0.04	0.24	-0.12	-0.09	-0.04	0.33	1.00								
GWL	0.97	-0.07	0.14	-0.72	0.31	-0.26	0.06	0.28	0.26	1.00									
N	0.21	0.04	0.90	0.29	0.91	-0.86	0.69	0.87	1.00										
CDG	0.26	0.03	0.82	0.13	0.70	-0.81	0.42	1.00											
Alluvium	0.03	0.06	0.76	0.42	0.58	-0.78	1.00												
Fill	-0.21	-0.03	-0.78	-0.25	-0.79	1.00													
Type	0.24	0.03	0.65	0.22	1.00														
Twin	-0.81	0.15	0.36	1.00															
Above	0.12	0.07	1.00																
Hori	-0.09	1.00																	
Chainge	1.00																		

Fig. 4 Correlation between settlement-inducing parameters and surface settlement

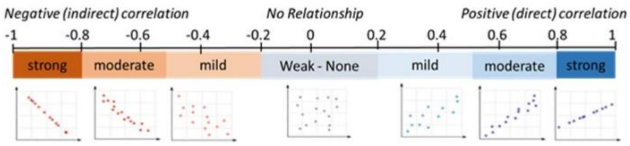

Fig. 5 Degrees of Pearson correlation

where n is the sample size. x_i and y_i are the individual sample points indexed with i. $\bar{x}$ and $\bar{y}$ are the sample mean. Ranges of linear relationship degree according to the Pearson correlation value is shown in Fig. 5 (Profillidis and Botzoris 2019).

Fig. 4 summarizes the evaluated correlation between the settlement-inducing parameters and the surface settlements. Outlier data were removed from the analysis because the Pearson correlation coefficient is adversely influenced by the existence of outliers. According to the results of correlation, the seven parameters show a relatively strong correlation (R > ±0.4) with the surface settlements. Among the geometrical parameters, the tunnel chainage and the twin tunnel parameter showed strong correlations, 0.54 and -0.44, respectively. This indicates the site in consideration is highly influenced by the twin tunnel formation and the existence of settlement trend along the tunnel chainage such as the initial driving zone near the launch station. The parameter of ground water represented the highest correlation, that is 0.58, among the geological parameters. Four TBM operating parameters, i.e., face pressure, advance rate, thrust and torque showed high correlations with the surface settlements, i.e., 0.49, -0.40, 0.52 and 0.56, which are consistent with the previous research results.

Fig. 4 illustrates not only the correlation between the effective parameters and the surface settlements, but also the correlation among the effective parameters. Analyzing the correlation among the effective parameters helps to comprehend the complex relationship of the surface settlement-inducing parameters. A trend of high correlation, represented in comparatively dark colors, was observed in the correlation between few parameters. Meanwhile, the horizontal distance parameter showed a relatively weak correlation, with all of correlation value less than 0.2, and represented in light whitish colors. Exceptionally high correlations (R > ±0.8) were observed between the N-value and the geological conditions, 0.91, -0.86 and 0.87, respectively, indicating that the soil strength parameter can be replaced with other settlement-inducing parameters such as the soil cover above the tunnel, soil type of tunnel path, layer thickness of fill and layer thickness of CDG. In most remaining parameters, mild correlations were observed, indicating that the settlement-inducing parameters have a complex and nonlinear relationship with each other. Because the Pearson analysis considers only a linear correlation, an additional trend analysis was performed to observe the nonlinear relationship between the settlement-inducing parameters and surface settlements.

4. Influence of settlement parameters on surface settlements

A general trend of the surface settlements along the tunnel chainage indicates extensive surface settlements developed in the initial driving section and around the chainage 400 m as shown in Fig. 6(a). While some heavings were observed in the initial driving section, an increasing trend of heaving was observed beyond 500 m. Fig. 6(b) shows the distribution of settlement monitoring points along the tunnel chainage in the transverse direction. The negative value of the horizontal distance indicates that the settlement monitoring points located in the right side of the tunnel

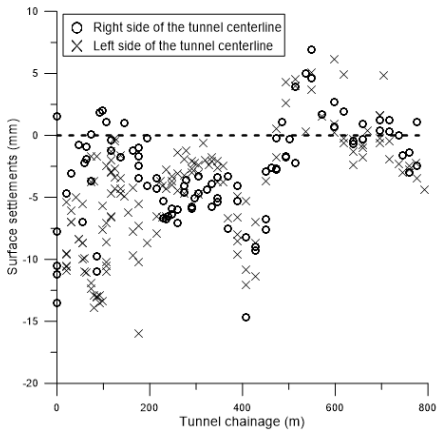

(a) Distribution of surface settlements

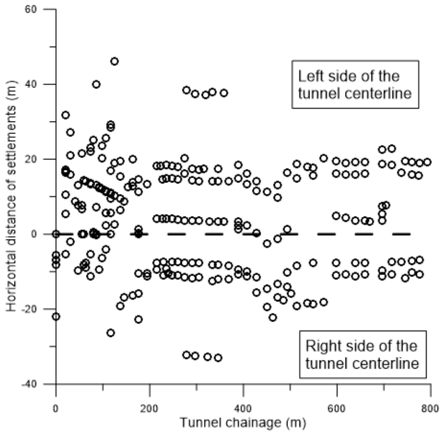

(b) Horizontal distance of settlement monitor point

Fig. 6 General trend of settlement monitoring points along tunnel chainage

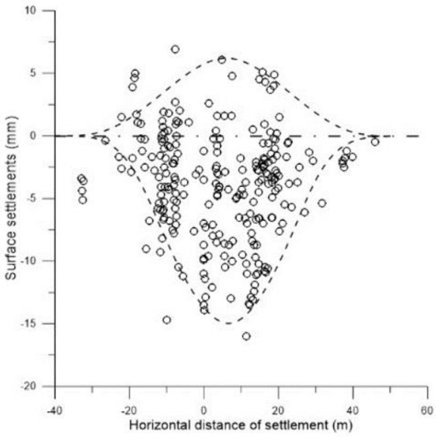

(a) Horizontal distance

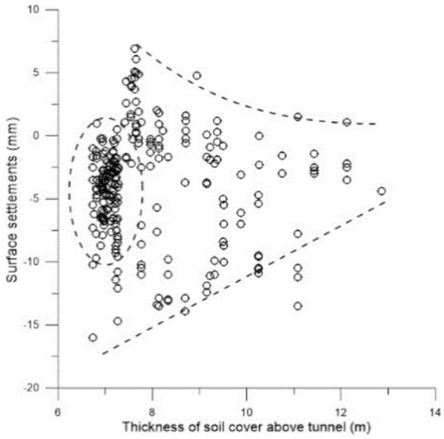

(b) Soil cover above tunnel

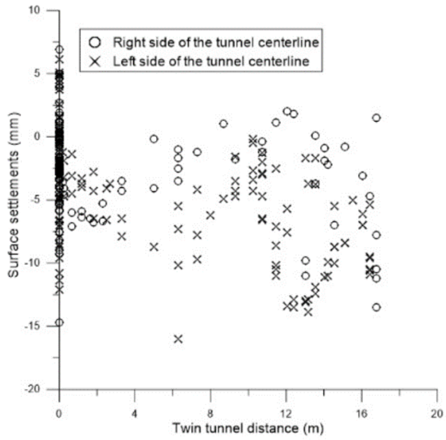

(c) Twin tunnel distance

Fig. 7 Correlation of surface settlements with geometrical parameters

centerline. In Fig. 6(a), heaving occurred near the chainage 100 m only at the right side of the tunnel centerline, while settlement up to 14 mm was monitored at the left side of the monitoring points for the same chainage. Such phenomenon is attributed to the twin tunnel effect, which is dominant in the initial driving section. In other words, either heaving or small settlement occurred at the right side of the tunnel, while larger settlement was observed at the left side of the tunnel centerline, which is the closer side to the down-track tunnel.

Even though there is no single explanation for the large magnitude of heaving occurred after the chainage 500 m, it is presumably attributed to two factors, i.e., the construction of an ancillary shaft and the excessive face pressure. The location of the shaft directly corresponds to the section extensive heaving within the chainage 500-600 m as shown in Fig. 1.

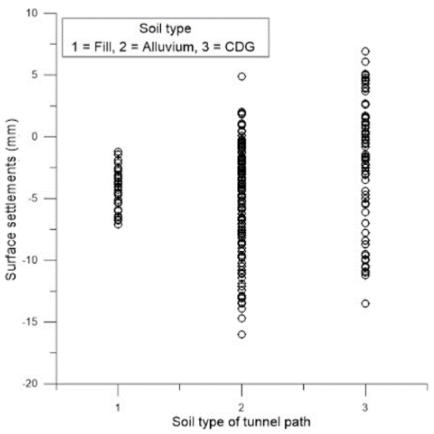

(a) Soil type at tunnel face

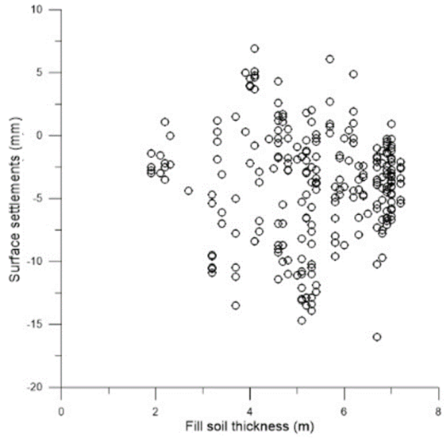

(b) Fill layer thickness at each section

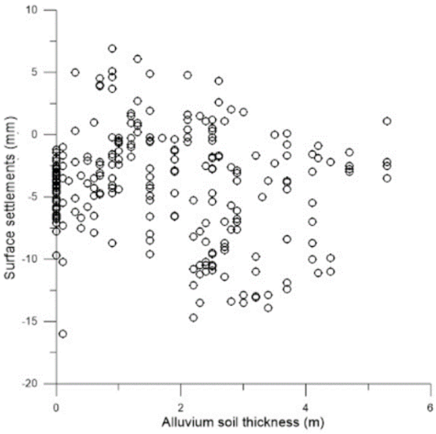

(c) Alluvium layer thickness at each section

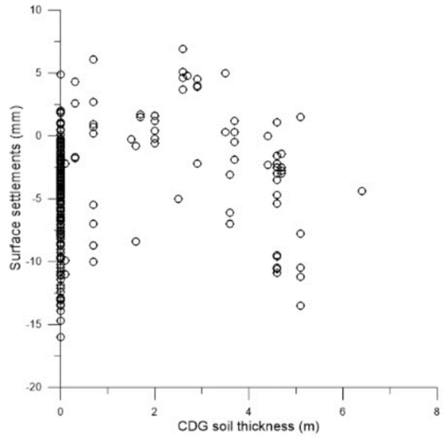

(d) CDG layer thickness at each section

Fig. 8 Correlation of surface settlements with soil type and soil layer thickness

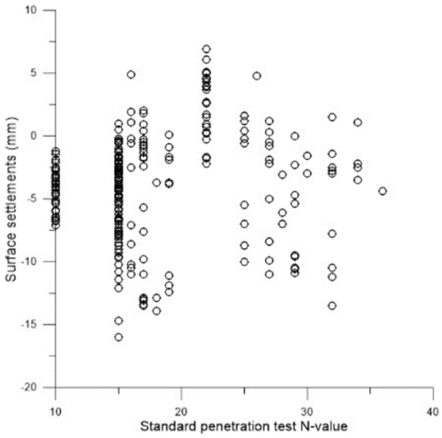

(a) Standard penetration test N-value

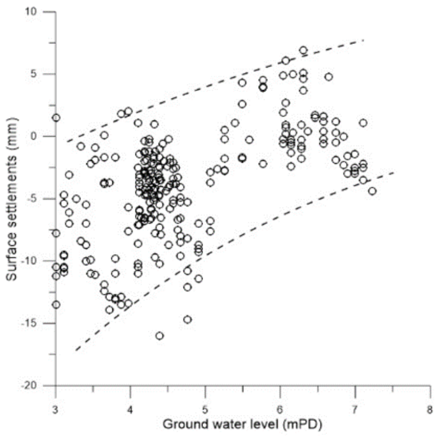

(b) Ground water level

Fig. 9 Correlation of surface settlements with geological parameters

4.1 Tunnel geometrical conditions

The relationship between the surface settlements and the tunnel geometrical parameters is analyzed in this section. The distribution of settlement and heaving measured at different horizontal distances of the transversal trough follows the normal Gaussian distribution as shown in Fig. 7(a). The center of normal curve is skewed to positive values, towards the center between the two twin tunnels, because of the twin tunnel effect. According to Fig. 7(b), both the maximum settlement and heaving were observed in case of thin soil cover conditions, less than 8 m, which is approximately equal to the tunnel diameter. The majority of surface settlements was concentrated in the range between 0 and 10 mm at the same thin soil cover condition. On the other hand, the magnitude of settlement and heaving

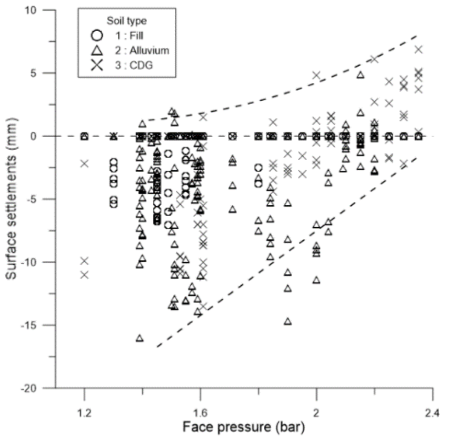

(a) Face pressure

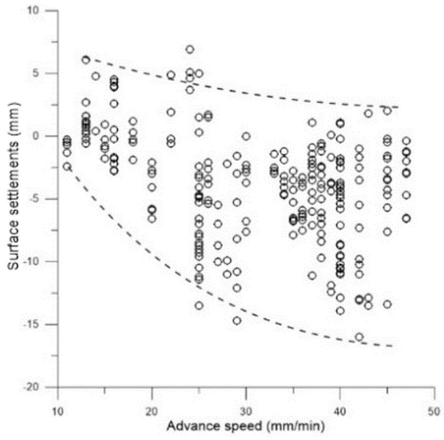

(b) Advance speed

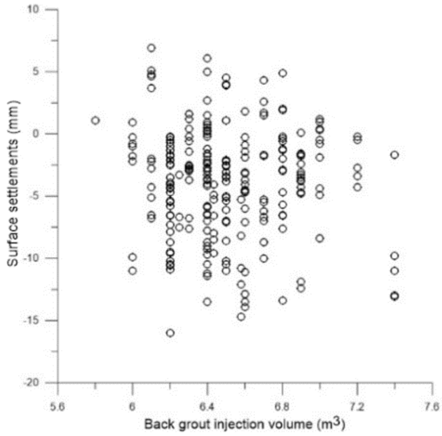

(c) Back grout injection volume

Fig. 10 Correlation of surface settlements with TBM operating conditions

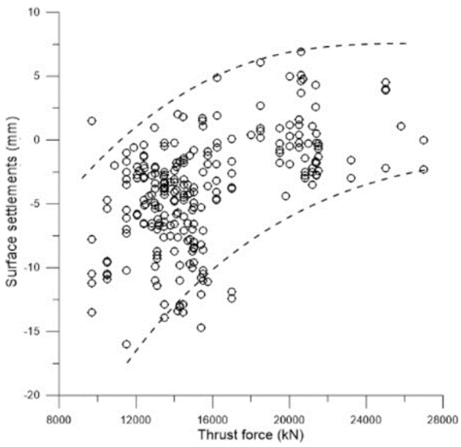

(a) Thrust force

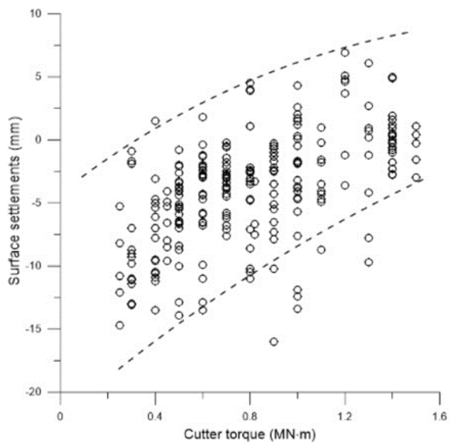

(b) Cutter torque

Fig. 11 Correlation of surface settlements with TBM operation

decreased with an increase in the thickness of soil cover above the tunnel. Considering such diversity of settlement data in the section with thin soil cover, it can be concluded that shallow-ground tunneling is more susceptible to the settlement-inducing factors than deep-ground tunneling.

The correlation of twin tunnel distances with the surface settlements is presented in Fig. 7(c). As discussed in the previous section, larger settlements were observed at the monitoring points located on the left side of the up-track tunnel, which is closer to the down-track tunnel, due to the twin tunnel effect.

4.2 Geological and geotechnical conditions

Soil types have unique features of geotechnical properties such as soil strength, stiffness and compressibility, which can be reflected to the induced

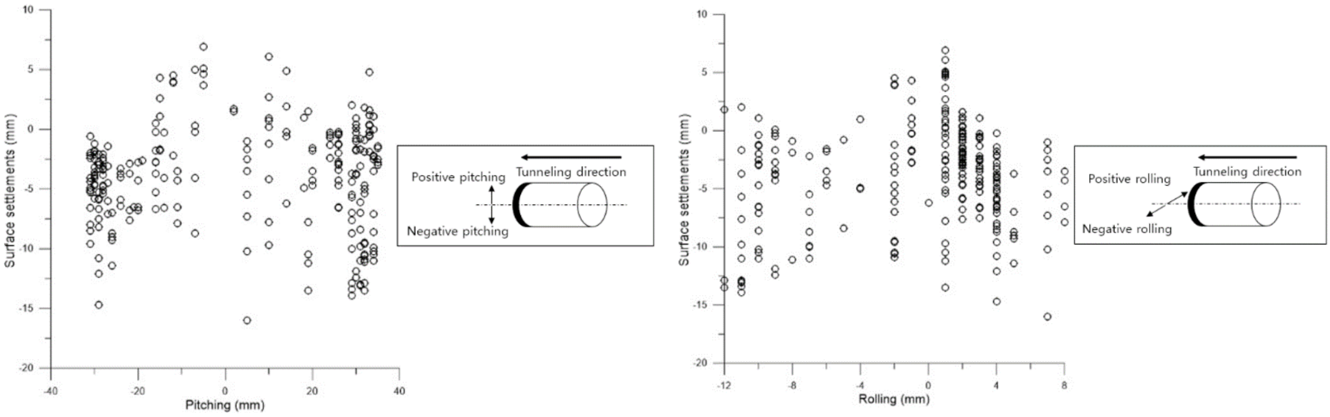

(a) Pitching (b) Rolling

Fig. 12 Correlation of surface settlements with TBM position

surface settlements in each soil layer. The soil types at the excavation face show a distinct tendency of the surface settlements and heaving as indicated in Fig. 8(a). The increased tendency of heaving is observed when the tunnel is passing through the alluvium and the CDG layer. 28 cases of heaving and 46 cases of settlement were recorded in the CDG layer, while 11 cases of heaving and 130 cases of settlement were recorded in the alluvium layer. While the CDG layer is more susceptible to heaving, with reaching up to 6.9 mm heaving, the alluvium layer is more susceptible to settlement, with the maximum settlement of 16 mm. Meanwhile, the surface settlements were well-controlled in the fill layer, with the settlement recorded less than 7.1 mm.

As the longitudinal geological profile is displayed in Fig. 1, the soil above the tunnel consists of a varing proportion of three soil types, i.e., fill, alluvium and CDG. Therefore, the effect of the distribution of soil layer thickness at each section on the surface settlements is illustrated in Figs. 8(b)-8(d). A significant scattering of settlements and heavings is observed, indicating that the other settlement-inducing parameters, such as the face pressure, the ground water parameter and the twin tunnel parameter are more influential than the soil sickness at each section.

The N-value obtained from the standard penetration test, representing the undrained strength of soil along the tunnel alignment, showed a weak correlation with the surface settlements in Fig. 9(a). Even though a number of heavings were observed around N=22, such heavings are presumably caused by unpredicted site-specific conditions. Fig. 9(b) indicates a strong correlation between the ground water level and the surface settlements. The magnitude of settlement decreases as the ground water level rises, leading to heavings at certain locations with the high ground water level, above 5.5 mPD. This trend may be attributable to exerting excessively high face pressure, which was initially designed for such adverse ground conditions with the high ground water levels.

4.3 TBM operating conditions

Correlations of the shield TBM operation conditions with the surface settlements are illustrated in Figs. 10-12.

Among the seven TBM operation parameters, strong correlation trends were observed in the following four parameters, i.e., face pressure, advance speed, thrust force and cutter torque.

As the primary mechanism of controlling the surface settlement during TBM tunneling, the face pressure indicated a noticeable trend in correlation with the surface settlements. Large surface settlements were monitored at the low face pressure, while smaller settlements and even heavings in some cases were observed at the high face pressure. Correlation of the surface settlements and the face pressure at different soil types showed a distinct trend as shown in Fig. 10(a). At the soft fill layer, the face pressure lower than 1.8 bar was applied. Since the surface settlements were successfully controlled at this soil type, the applied face pressure was proven to be adequate. At the alluvium and CDG soil layer, a wide range of face pressure was applied, from 1.2 to 2.35 bar. Larger surface settlements were observed at the alluvium layer indicating the surface settlements at the alluvium layer is effected by other settlement-inducing parameters. Unlike the other two soil types, extensive heavings were observed in the CDG layer particularly at the high face pressure level. Because heavings were rarely observed at the same face pressure level in the alluvium layer, which locates on top of the CDG layer, the heavings observed in the CDG layer should be related to other settlement-inducing parameters.

A distinctive relation between the advance speeds and the surface settlements shows decreasing settlements at a low level of advance speed in Fig. 10(b). The injected volume of backfill grout was not found to correlate with the surface settlements as shown in Fig. 10(c). Moreover, significantly scattered settlements were observed in the range of injected volume of backfill grout.

Both the thrust force and the cutter torque were inversely proportional to the surface settlements as shown in Fig. 11, where smaller surface settlements or heavings in some cases were observed at high levels of the thrust force and cutter torque. The thrust force has a close relationship with the face pressure and the advance speed because high thrust force is understandably required for higher face pressure and faster advance speed. In Fig. 11(a), while settlements larger than 10 mm were observed between 10,000 kN and 18,000 kN of the thrust force, settlements were controlled below 5 mm at the thrust force above 18,000 kN. In the case of cutter torque in Fig. 11(b), the linearly decreasing trend of the surface settlements was indicated in the entire range of cutter torque, with only a few outliers around 1 MN·m that were possibly induced by other settlement-inducing factors.

In general, the pitching of TBM shield enlarges both the upper and lower annular gap between the shield and ground. The surface settlements increased at the high pitching, i.e., higher than ±30 mm, as shown in Fig. 12(a). While no heavings were observed in the negative pitching of -30 mm, i.e., tunneling downwards, a few heavings were monitored in the positive pitching. No specific correlation was found between the rolling and surface settlements as shown in Fig.12 (b).

5. Conclusions

This paper analyzed correlations between the settlement -inducing parameters and the surface settlements monitored from the twin shield TBM construction site in Hong Kong. An extensive database of surface settlement-inducing parameters and observed surface settlements is constructed.

For determining the effective parameters, the distribution and general trend of each parameter are scrutinized along with the Pearson correlation coefficient. The correlation analyses demonstrate several effective or explanatory parameters on the surface settlements. The key findings of this study can be summarized as follows.

1) The Pearson correlation analysis revealed the high linear correlation of seven surface settlement-inducing parameters to the surface settlements, i.e., chainage length, twin tunnel parameter, ground water level, face pressure, advance rate, thrust and torque.

2) In the considered site, the twin tunnel effect was found dominant in the initial driving section. During the initial driving, extensive settlements up to 14 mm were observed at the left side of the tunnel centerline, while heavings were observed at the right side of the same chainage. The Pearson correlation analysis between the twin tunnel parameter and the surface settlements indicates -0.44, which is relatively high compared to other parameters. Such phenomenon highlights that the effect of geometrical parameters on the surface settlement are critical in the target tunneling site.

3) A wide range of settlements and heavings was observed in the thin soil cover condition where both the maximum settlement and heaving were observed. Although the Pearson correlation analysis indicated only the mild correlation of -0.07, between the soil thickness above the tunnel and surface settlements, a decreasing tendency of the magnitude of settlements and heavings is clear according to the plotted graph. Therefore, the soil thickness should be considered as an effective parameter to the surface settlements.

4) A clear trend of the surface settlements was observed in the soil type of tunnel path. While only small settlements were observed in the fill layer, widely scattered settlement data were obtained in both the alluvium soil layer and the CDG layer. By analyzing the portion of the recorded heavings and settlements, it can be concluded that the CDG layer is more susceptible to heaving, while the alluvium layer is susceptible to extensive settlements. In addition, a proportional relation between the ground water level and surface settlements was observed. Therefore, the soil type and ground water level were found to be effective to the surface settlements.

5) Four TBM operation parameters, i.e., the face pressure, advance speed, thrust force and cutter torque, showed a relevant correlation with the surface settlements. While a proportional relation was found in most operation parameters, an inversely proportional relationship was observed in the case of advance speed. Such relationship is also consistent with the Pearson correlation analysis result, with 0.49, -0.40, 0.52 and 0.56 respectively, indicating these operation parameters are influential in the surface settlements.

6) Throughout the entire settlement-inducing parameter data, a large degree of scattering was encountered, which indicates that the surface settlements were induced as the result of a complex non-linear combination of multiple settlement-inducing parameters. To overcome such complicated challenge, further advanced approaches such as the artificial intelligence methods are required for the data analysis.

Acknowledgments

This research was supported by Basic Science Research Program through the National Research Foundation of Korea (NRF) funded by the Ministry of Education (2019R1A2C2086647).

References

Ahangari, K., Moeinossadat, S.R. and Behnia, D. (2015), “Estimation of tunnelling-induced settlement by modern intelligent methods”, *Soils Found.*, **55**(4), 737-748. https://doi.org/10.1016/j.sandf.2015.06.006.

Atkinson, J.H. and Potts, D.M. (1977), “Subsidence above shallow tunnels in soft ground”, *J. Geotech. Geoenviron. Eng.*, **103**, 307-325.

Attewell, P.B., Yeates, J. and Selby, A.R. (1986), *Soil Movements Induced by Tunnelling and Their Effects on Pipelines and Structures*, Blackies and Sons Ltd, London, U.K.

Bouayad, D. and Emeriault, F. (2017), “Modeling the relationship between ground surface settlements induced by shield tunneling and the operational and geological parameters based on the hybrid PCA/ANFIS method”, *Tunn. Undergr. Sp. Technol.*, **68**, 142-152. https://doi.org/10.1016/j.tust.2017.03.011.

Chen, R.P., Zhang, P., Kang, X., Zhong, Z.Q., Liu, Y. and Wu, H.N. (2019), “Prediction of maximum surface settlement caused by EPB shield tunneling with ANN methods”, *Soils Found.*, **59**(2), 284-295. https://doi.org/10.1016/j.sandf.2018.11.005.

Ding, W.Q., Yue, Z.Q., Tham, L.G., Zhu, H.H., Lee, C.F. and Hashimoto, T. (2004), “Analysis of shield tunnel”, *Int. J. Numer. Anal. Meth. Geomech.*, **28**(1), 57-91. https://doi.org/10.1002/nag.327.

Ding, Z. Wei, X.J. and Wei, G. (2017), “Prediction methods on tunnel-excavation induced surface settlement around adjacent building", *Geomech*. *Eng*., **12**(2), 185-195. https://doi.org/10.12989/gae.2017.12.2.185.

Eskandari, F., Goharrizi, K.G. and Hooti, A. (2018), "The impact of EPB pressure on surface settlement and face displacement in intersection of triplet tunnels at Mashhad metro", *Geomech*. *Eng*., **15**(2), 769-774. https://doi.org/10.12989/gae.2018.15.2.769.

Hasanipanah, M., Noorian-Bidgoli, M., Jahed Armaghani, D. and Khamesi, H. (2016), "Feasibility of PSO-ANN model for predicting surface settlement caused by tunneling", *Eng*. *Comput*., **32**(4), 705-715. https://doi.org/10.1007/s00366-016-0447-0.

Kasper, T. and Meschke, G. (2004), "A 3D finite element simulation model for TBM tunnelling in soft ground", *Int*. *J*. *Numer*. *Anal*. *Meth*. *Geomech*., **28**(14), 1441-1460. https://doi.org/10.1002/nag.395.

Kim, C.Y., Bae, G.J., Hong, S.W., Park, C.H., Moon, H.K. and Shin, H.S. (2001), "Neural network based prediction of ground surface settlements due to tunneling", *Comput*. *Geotech*., **28**(6-7), 517-547. https://doi.org/10.1016/S0266-352X(01) 00011-8.

Kim, K., Oh, J.Y., Lee, H., Kim, D. and Choi, H. (2018), "Critical face pressure and backfill pressure in shield TBM tunneling on soft ground", *Geomech*. *Eng*., **15**(3), 823-831. https://doi.org/10.12989/gae.2018.15.3.823.

Kohestani, V.R., Bazargan-Lari, M.R. and Asgari-marnani, J. (2017), "Prediction of maximum surface settlement caused by earth pressure balance shield tunneling using random forest", *J*. *AI Data Min*., **5**(1), 127-135. https://doi.org/10.22044 /jadm.2016.748.

Leca, E. and New, B. (2007), "Settlements induced by tunneling in soft ground", *Tunn*. *Undergr*. *Sp*. *Technol*., **22**(2), 119-149. https://doi.org/10.1016/j.tust.2006.11.001.

Loganathan, N. and Poulos, H.G. (2002), "Analytical prediction for tunneling-induced ground movements in clays", *J*. *Geotech*. *Geoenviron*. *Eng*., **124**(9), 846-856. https://doi.org/10.1061/(asce)1090-0241(1998)124:9(846).

Mair, R.J. (1983), "Geotechnical aspects of soft ground tunneling", *Proceedings of the International Symposium on Construction Problems in Soft Soils*, Singapore.

Melis, M., Medina, L. and Rodríguez, J.M. (2002), "Prediction and analysis of subsidence induced by shield tunnelling in the Madrid Metro extension", *Can*. *Geotech*. *J*., **39**(6), 1273-1287. https://doi.org/10.1139/t02-073.

Neaupane, K.M. and Adhikari, N.R. (2006), "Prediction of tunneling-induced ground movement with the multi-layer perceptron", *Tunn*. *Undergr*. *Sp*. *Technol*., **21**(2), 151-159. https://doi.org/10.1016/j.tust.2005.07.001.

O'Reilly, M.P. and New, B.M. (1982), "Settlements above tunnels in the United Kingdom - their magnitude and prediction", *Proceedings of the 3rd International Symposium on Tunnelling'82*, Brighton, U.K., June.

Park, K.H. (2005), "Analytical solution for tunnelling-induced ground movement in clays", *Tunn*. *Undergr*. *Sp*. *Technol*., **20**(3), 249-261. https://doi.org/10.1016/j.tust.2004.08.009.

Peck, R.B. (1969), "Deep excavations and tunneling in soft ground", *Proceedings of the 7th International Conference on Soil Mechanics and Foundation Engineering*, Mexico City, Mexico.

Profillidis, V.A. and Botzoris, G.N. (2019), *Chapter 5 - Statistical Methods for Transport Demand Modeling*, in *Modeling of Transport Demand*, Elsevier.

Rezaei, A.H., Shirzehhagh, M. and Golpasand, M.R.B. (2019), "EPB tunneling in cohesionless soils: A study on Tabriz Metro settlements", *Geomech*. *Eng*., **19**(2), 153-165. https://doi.org/10.12989/gae.2019.19.2.153.

Sagaseta, C. (1987), "Analysis of undraind soil deformation due to ground loss", *Geotechnique*, **37**(3), 301-320. https://doi.org/10.1680/geot.1987.37.3.301.

Santos, O.J. and Celestino, T.B. (2008), "Artificial neural networks analysis of São Paulo subway tunnel settlement data", *Tunn*. *Undergr*. *Sp*. *Technol*., **23**(5), 481-491. https://doi.org/10.1016/J.TUST.2007.07.002.

Suwansawat, S. and Einstein, H.H. (2006), "Artificial neural networks for predicting the maximum surface settlement caused by EPB shield tunneling", *Tunn*. *Undergr*. *Sp*. *Technol*., **21**(2), 133-150. https://doi.org/10.1016/j.tust. 2005.06.007.

Verruijt, A. and Booker, J.R. (1998), "Surface settlements due to deformation of a tunnel in an elastic half plane", *Geotechnique*, **48**(5), 709-713.

Yagiz, S., Gokceoglu, C., Sezer, E. and Iplikci, S. (2009), "Application of two non-linear prediction tools to the estimation of tunnel boring machine performance", *Eng*. *Appl*. *Artif*. *Intell*., **22**(4-5), 808-814. https://doi.org/10.1016/j.engappai.2009.03.007.

Zhang, L.M., Wu, X.G., Ji, W.Y. and AbouRizk, S.M. (2017), "Intelligent approach to estimation of tunnel-induced ground settlement using wavelet packet and support vector machines", *J*. *Comput*. *Civ*. *Eng*., **31**(2), 04016053. https://doi.org/10.1061/(asce)cp.1943-5487.0000621.

CC